LETTERS

# Rank clocks

Michael Batty[1]

**Many objects and events, such as cities, firms and internet hubs, scale with size[1–4] in the upper tails of their distributions. Despite intense interest in using power laws to characterize such distributions, most analyses have been concerned with observations at a single instant of time, with little analysis of objects or events that change in size through time (notwithstanding some significant exceptions[5–7]). It is now clear that the evident macro-stability in such distributions at different times can mask a volatile and often turbulent micro-dynamics, in which objects can change their position or rank-order rapidly while their aggregate distribution appears quite stable. Here I introduce a graphical representation termed the 'rank clock' to examine such dynamics for three distributions: the size of cities in the US from AD 1790, the UK from AD 1901 and the world from 430 BC. Our results destroy any notion that rank–size scaling is universal: at the micro-level, these clocks show cities and civilizations rising and falling in size at many times and on many scales. The conventional model explaining such scaling on the basis of growth by proportionate effect cannot replicate these micro-dynamics, suggesting that such models and explanations are considerably less general than has hitherto been assumed.**

I begin with the US city size distributions compiled[8] for the populations of the largest 100 cities from AD 1790 to AD 2000 using the decennial Population Census. City sizes are represented as rank–size distributions after Zipf, where population in city $i$ at time $t$, $P_i(t)$, is ordered against its rank $r_i(t)$ and plotted logarithmically to give an immediate visualization of scaling[9]. The relative stability of these rankings is clear from the plots in Fig. 1a but the switch in rankings, with many cities entering and leaving the top 100, is completely hidden. Over this 210 yr period, there are 266 cities that at some stage belong to the top 100; from 1840 when the number of cities first reached 100, only 21 remain in 2000. On average, it takes 105 yr for 50% of cities to appear or disappear from the top 100, while the average change in rank order for a typical city in each 10 yr period is 7 ranks. If the distributions are collapsed onto one another, there is only an 18% difference between any of their rank orders. This contrasts with a typical switch in rank orders, which is also illustrated in Fig. 1a, where I plot the '1950' ranks using '2000' population values.

To visualize these micro-dynamics, I first plot trajectories in Fig. 1b based on the rank and size of each city in the rank–size space where each city is coloured according to its rank order and the time when it first appears in the top 100. These trajectories are ordered so that greater changes in rank overlay lower ones. Although cities that do not change their rank show up clearly as vertical lines, this plot is confusing. I therefore propose a 'rank clock', where rank orders are plotted for each city in temporal clockwise direction with the highest rank at the centre and the lowest on the circumference. This provides an immediate visualization of the dynamics, as I show for the US data in Fig. 1c. To develop meaningful analysis on the clock, I measure various displacements of rank, but first extract significant city trajectories as in Fig. 1d. New York City has been the top rank (at the clock's centre) since 1790, but the clock reveals how large cities such as Chicago, Los Angeles and Houston enter the system as population diffuses across the US, how cities in the original 13 colonies such as Richmond and Charleston fall out of favour, and how cities in the northeast 'rust-belt' such as Buffalo slowly decline in rank.

To complement the US data, I have constructed clocks for two other very different data sets. The US data are based on the rapid growth of key cities in the New World, and represent the transition from an essentially agrarian society to an industrial one. The original 24 cities in 1790 comprise only 5% of the US population (~200,000), whereas in 2000, the top 100 cities constitute 20% (~55 million). The UK data, taken from a reworking of the decennial Census data into 458 urban places[10], illustrates a population growing from 37 million to 57 million over the period AD 1901 to AD 2001. The third set is based on Chandler's 4,000 yr world history of urban growth[11], from which I have culled and added data to the top 50 cities from 430 BC to AD 2000. There are 390 distinct cities in this data that grow from about 3 million in total to almost 600 million over the period. Like the US data, this reveals the massive transition to industrialization but only at the very end of the time series. Other key transitions from the classical era to the Dark Ages, the importance of China and Japan, the ebb and flow of urban populations in the Middle Ages, and the emergence of the modern era, are all reflected in this data. Details are contained in the Supplementary Information.

Rank–size distributions and rank clocks are shown for the UK and world data in Fig. 2. The UK rank–size profiles show scaling in the upper tail as the number of urban places in this data set is fixed. In the UK data, of the top 100 cities in 1901, 73 remain in these top ranks in 2001. The change in rank order in each 10 yr period for an average city is only 14 out of a total of 458 cities, which is less than half the US rate. In the world data, no cities in the top 50 in 430 BC remain in the top 50 in the year 2000, while from the Fall of Constantinople in 1453, only 6 cities from that era now appear in the top 50 (in 2000). The cities that show the greatest longevity through their being in the top 50 over the 2,430 yr period are perhaps surprising: Suzhou (2,158 yr), Nanking (2,080 yr), Wuchang (1,850 yr), Benares (1,780 yr), Rayy (1,630 yr) and Rome (1,530 yr). Paris (525 yr) is 77th out of 390 cities.

The half life for cities in this data set remaining in the top 50 is ~200 yr, almost twice as long as for the US data. Comparing the patterns in the three clocks in Figs 1 and 2, visual intuition suggests that changes in rank are smoothest in the UK data, more volatile and complex in the US, while most volatile in the world data where large changes in rank seem to dominate all historical periods. A more detailed sample of this micro-dynamics is shown in the clock in Fig. 3, where 7 'typical' cities are plotted for the world data, each showing a different pattern of rank change, suggesting a possible basis for future classification of city types based on their local dynamics[12].

To compare these three systems, I reduce each set of cities to the top 50. These of course generate different rank clocks (shown in the Supplementary Information) in the US and UK systems, as I am now dealing with the top 50 cities from 266 US and 458 UK cities. Throughout I am also making the assumption that a city that exists at times $t-1$ and $t$ in the top 50 remains in that list regardless of the length of time between $t-1$ and $t$. For the world data set where time

[1]Centre for Advanced Spatial Analysis, The Bartlett School, University College London, 1–19 Torrington Place, London WC1E 6BT, UK.

periods vary substantially in length, this complicates the analysis, for cities might hop in and out of the top 50 during long time intervals.

The rank shifts[13] are defined as distances $d_i(t) = |\, r_i(t) - r_i(t-1)\,|$, which exist only if the city in question is in the top 50 at each time period within which $N_i(t)$ such cities comprise the common set $\Omega(t)$. These distances can be plotted on the clock, as can the average shift per time $d(t) = \sum_{i\in\Omega(t)} |\, r_i(t) - r_i(t-1)\,| \Big/ N_i(t)$, which enables analysis of the extent to which the system is converging or diverging in terms of rank shift[14]. The average shift over all time periods $T$ is defined as $d = \sum_t d(t) \Big/ T$. If there are no shifts, then all these distances are zero, while the maximum average shift that can take place at any time is $d(t) < n/2$ where $n = 50$, the total number of cities in the list.

These distances are plotted in Fig. 4a–c. The world system is clearly the most volatile, with an overall shift $d$ of 14.27 and with the average $d(t)$ indicating bigger shifts in the classical era and until around the year AD 1000. After that, there is a gradual reduction in shift until the Industrial Revolution. For the US data, the overall shift is much lower with $d$ at 4.67, with the average $d(t)$ being largest between 1830 and 1890, the period of greatest city expansion in the US. I would expect the UK to have much lesser volatility from the earlier analysis, but once the city set is restricted to the top 50, changes in rank ($d$ at 4.22) are only a little less than for the US case. The UK was effectively locked into its current urban settlement pattern by 1901, and rank shifts in the last century are greatest in the 1950s and 1960s, a period of rapid suburbanization[15].

My second analysis involves defining growth rates and examining their trajectories using the rank clock. These rates will be split into those associated with the growth and the change in the share of population in cities. First I define the growth rate for each city $i$ at time $t$, $\lambda_i(t)$, as $P_i(t)/P_i(t-1)$, from which $P_i(t) = \lambda_i(t)\ P_i(t-1)$ and then define population shares as $p_i(t) = P_i(t)/P(t)$ where total population is $P(t) = \sum_i P_i(t)$. The expected growth rate for cities $\lambda(t)$ is:

$$\lambda(t) = \sum_i p_i(t)\lambda_i(t) = \sum_i p_i(t)\frac{P_i(t)}{P_i(t-1)} = \left\{\frac{P(t)}{P(t-1)}\right\}\left\{\sum_i p_i(t)\frac{p_i(t)}{p_i(t-1)}\right\} \quad (1)$$

where the overall growth $\Gamma(t)$ and expected shift in population shares $\vartheta(t)$ are the first and second terms on the second line of equation (1), respectively. A more workable form is based on the logarithmic growth rate $\log\lambda_i(t) = \log[P_i(t)/P_i(t-1)]$, whose expected value is an information statistic defined as:

$$I\,[\lambda(t)] = \sum_i p_i(t)\log\lambda_i(t) = \sum_i p_i(t)\log\frac{P_i(t)}{P_i(t-1)} = \log\frac{P(t)}{P(t-1)} + \sum_i p_i(t)\log\frac{p_i(t)}{p_i(t-1)} \quad (2)$$

The log of overall growth $I\,[\Gamma(t)]$ and expected log of the shares $I\,[\vartheta(t)]$ are the first and second terms on the second line of equation (2). The second term is an information difference, which holds the key to further analysis through decomposition into growth and change at different spatial scales, thereby enabling different systems to be integrated through a hierarchy of information entropies[16–18].

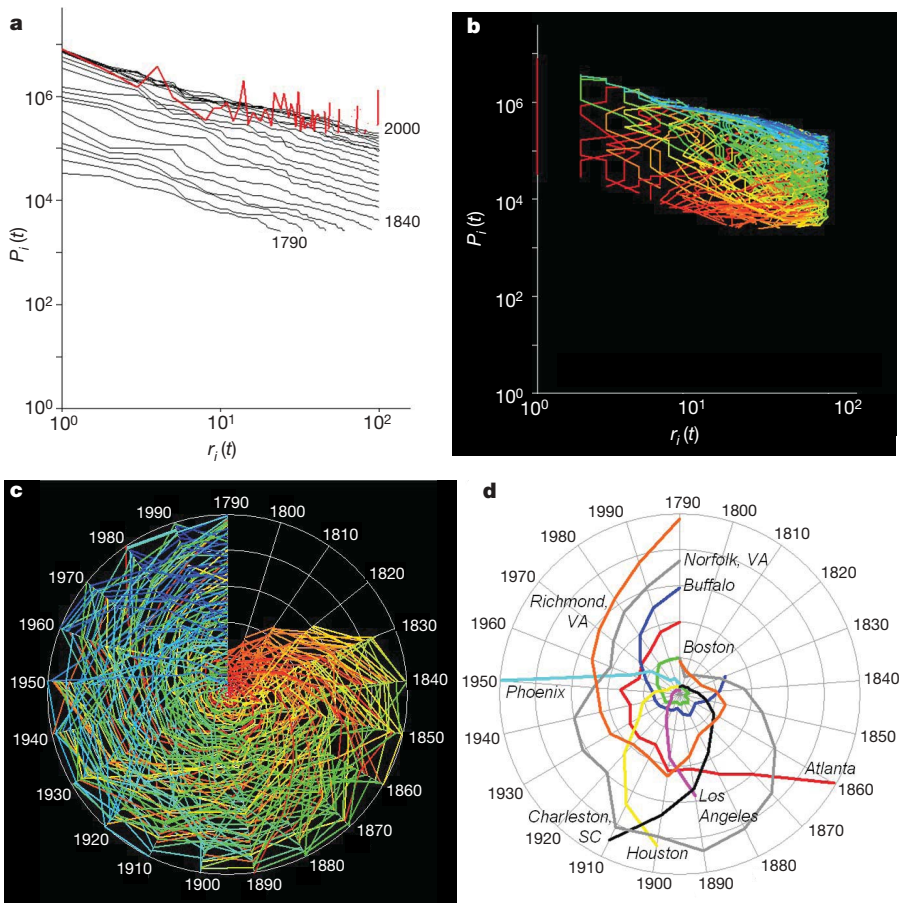


**Figure 1 | Rank size and rank clocks for the US urban system 1790–2000.** **a**, Zipf plots of the top 100 cities. Red indicates the rank of cities in 1950 using populations for 2000. **b**, Trajectories of each city in rank–size space with New York City rank 1 throughout. **c**, The rank clock, with each axis running from rank 1 at the centre to 100 on the circumference, and cities coloured by date of entry from 1790 (red) to 2000 (blue). **d**, Sample city trajectories.

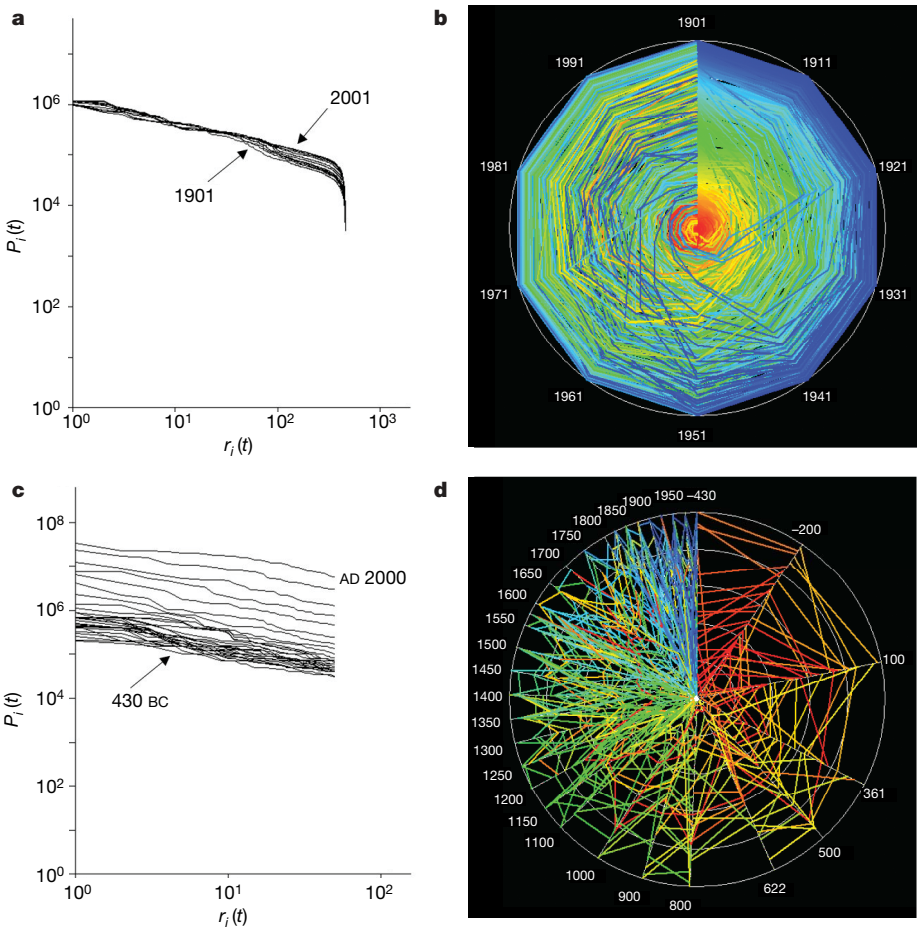


**Figure 2 | Rank size and rank clocks for the UK and world urban systems.** **a**, **b**, The Zipf plot (**a**) and the rank clock (**b**) for the UK, with each clock axis from rank 1 to 458. **c**, **d**, The Zipf plot (**c**) and the rank clock (**d**) for the world, with each clock axis from rank 1 to 50.

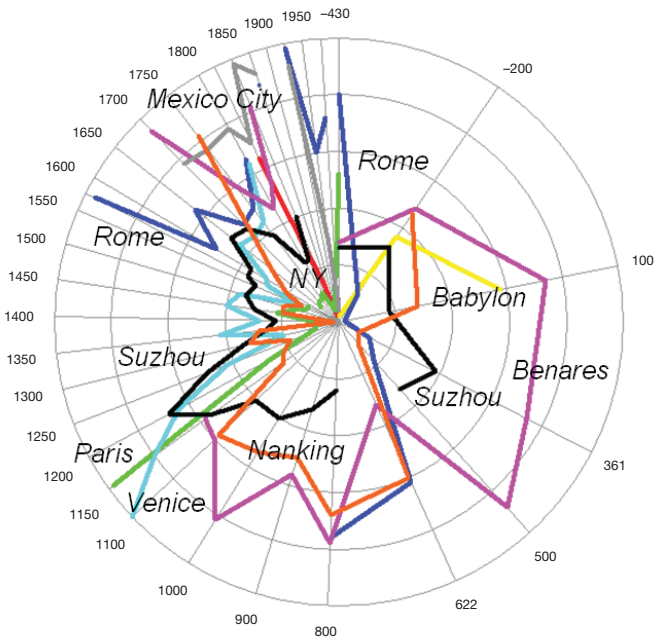


**Figure 3 | Trajectories of a sample of world cities from 430 BC to AD 2000.** Note the dominance of Rome until modern times, and the importance of the Chinese cities Nanking and Suzhou. From 1600 onwards, the volatility of the clock increases as cities of the early modern period and the Industrial Revolution are replaced in the top 50 by cities in the developing world.

These growth and information statistics reflect the balance between overall change and the shift and share in rank and population size, which in its simplest additive form is expressed in the expected log of city growth rates in equation (2). The growth and information components averaged over all time periods for each data set are shown in Table 1, where it is clear that for the world and UK systems, the averages $\vartheta$ and $I[\vartheta]$ are very small, implying relatively little contribution to overall growth, which mainly comes from $\Gamma$ and $I[\Gamma]$. In contrast, there is greater shift and overall growth in the US system. However, the UK has been a low growth city system over the entire data period whereas the world system had relatively low growth from 430 BC to about AD 1600 when it began to take off. These patterns are very clear in the trajectories of the three growth components, which are plotted in rank clock form for all three systems in Fig. 4d. The information statistics mirror these trajectories. There we observe for the world system that the $\vartheta(t)$ and $I[\vartheta(t)]$ make very little contribution to the total change while $\Gamma(t)$ and $I[\Gamma(t)]$ dominate, with the significant periods being the early Dark Ages from the collapse of the Roman Empire to around 500, and the Industrial Revolution which merges into the current era of globalization beginning around 1800[19]. In the UK system, the statistics pick up the recession period 1930–40 and the relatively low growth era of the 1970s. Lastly, the US urban system shows much greater growth and population shifts in the nineteenth century with specific shifts in population in the 1860s and relatively low periods of growth in the 1820s, the 1930s and 1940s, and the 1980s.

The information generated on the micro-dynamics of rank size can be used to examine the consistency of the widely accepted model used to generate growth and change in systems that scale[1,20–22]. This model is based on proportionate random growth, first suggested by Gibrat[23],

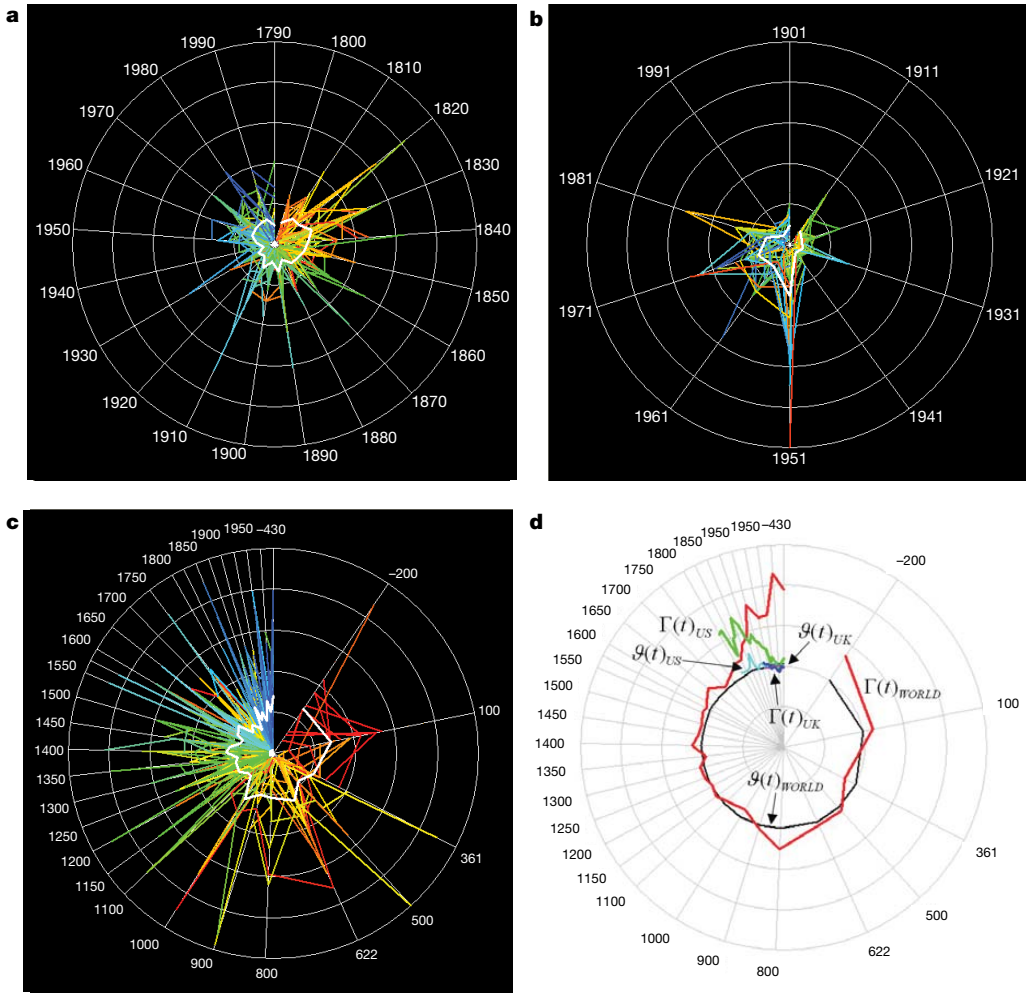


**Figure 4 | Distance clocks and growth rates.** **a**–**c**, Distance clocks for the top 50 cities for the US (**a**), the UK (**b**) and the world (**c**), coloured according to when each city enters the rank order from the earliest in red to the latest in blue, and with greatest changes in distance overlaying lesser. **d**, The shift-share growth clock. All axes are from rank 1 to 50 for the clocks in **a**, **b** and **c**, and from 0 (centre) to 2.5 (circumference) for **d**.

subject to a lower bound $P_{\min}(t)$ below which populations cannot fall. For $n$ cities, $P_i(t) = [\Gamma + \varepsilon_i(t)]\, P_i(t-1)$ with $P_i(t) > P_{\min}(t)$ where $\varepsilon_i(t)$ is a random value chosen from a normal distribution, and $P_{\min}(t)$ is a fixed proportion of the average $P(t)/n$ of the total population[24]. With 1,500 cities and using a constant ten year growth rate of 1.126 discounted to each yearly time step, I have run the model for $T = 2{,}500$ steps, which mirrors the population change in Chandler's world data set. The biggest differences between the simulated and three real data sets are the low values of the population shift-shares with $\vartheta = 1.00061$ and $I[\vartheta] = 1.00031$. The macro- and micro-dynamics of this simulation are shown in the Supplementary Information, from which it is clear that the rank clock has some similarities with that associated with the world data set, whereas the distance clock is similar to the US clock.

**Table 1 | Distance, growth and information statistics**

| Component | US | World | UK | Gibrat's model |
|---|---|---|---|---|
| $d$ | 4.6675 | 14.2773 | 4.22049 | 9.4853 |
| $\lambda = \sum_i \lambda(t) \Big/ T$ | 1.3787 | 1.1311 | 1.0044 | 1.3441 |
| $\Gamma = \sum_i \Gamma(t) \Big/ T$ | 1.3122 | 1.1256 | 0.9991 | 1.3433 |
| $\vartheta = \sum_i \vartheta(t) \Big/ T$ | 1.0456 | 1.0042 | 1.0054 | 1.0006 |
| $I[\lambda] = \sum_i I[\lambda(t)] \Big/ T$ | 0.2770 | 0.1032 | 0.0010 | 0.2942 |
| $I[\Gamma] = \sum_i [\Gamma(t)] \Big/ T$ | 0.2572 | 0.1012 | -0.0017 | 0.2939 |
| $I[\vartheta] = \sum_i I[\vartheta(t)] \Big/ T$ | 0.0198 | 0.0020 | 0.0027 | 0.0003 |

See text for details of quantities in the leftmost column. All rates are normalized to 10 yr time intervals.

It is clear however that this model is not able to generate the unique events associated with a turbulent world history in the rise and fall of cities and civilizations[19], nor is it able to mirror change over shorter time periods. Although Gibrat's model does generate universal scaling behaviour for city size distributions, its micro-dynamics is very different from that which is revealed using the rank clocks. Models of proportionate random growth generating scale-free effects are now being explored for networks, and preliminary analysis of their historical dynamics can be informed using rank clocks[25]. To test these ideas further, much larger temporal data sets—such as clusters of internet hubs and websites, firm sizes, scientific citation networks, individual income distributions, and short lived epidemics—would thus appear to be excellent candidates for analysis using rank clocks.

**Received 12 May; accepted 27 September 2006.**

1. Blank, A. & Solomon, S. Power laws in cities population, financial markets and internet sites: Scaling and systems with a variable number of components. *Physica A* **287**, 279–288 (2000).
2. Gabaix, X. & Ioannides, Y. M. in *Handbook of Regional and Urban Economics* Vol. 4 (eds Henderson, V. & Thisse, J-F.) 2341–2378 (North-Holland, Amsterdam, 2004).

3. Axtell, R. L. Zipf distribution of U.S. firm sizes. *Science* **293,** 1818–1820 (2001).
4. Adamic, L. A. & Huberman, B. A. Zipf's law and the internet. *Glottometrics* **3,** 143–150 (2002).
5. Stanley, M. H. R. *et al.* Scaling behavior in the growth of companies. *Nature* **379,** 804–806 (1996).
6. White, D. R., Kejzar, N., Tsallis, C. & Rozenblat, C. *Generative Historical Model of City-Size Hierarchies: 430BCE–2005* (ISCOM Working Paper, Institute of Mathematical Behavioral Sciences, University of California, Irvine, CA, 2005).
7. Barabasi, A-L. The origin of bursts and heavy tails in human dynamics. *Nature* **435,** 207–211 (2005).
8. Gibson, C. *Population of the 100 Largest Cities and Other Urban Places in the United States: 1790 to 1990* (Population Division Paper 27, US Bureau of the Census, Washington DC, 1998).
9. Zipf, G. K. *Human Behavior and the Principle of Least Effort* (Addison-Wesley, Cambridge, Massachusetts, 1949).
10. CDU census website. ⟨http://census.ac.uk/cdu/⟩ (accessed 8 August, 2006).
11. Chandler, T. *Four Thousand Years of Urban Growth: An Historical Census* (Edward Mellon, Lampeter, UK, 1987).
12. Ioannides, Y. M. & Overman, H. G. Zipf's law for cities: An empirical examination. *Reg. Sci. Urban Econ.* **33,** 127–137 (2003).
13. Havlin, S. The distance between Zipf plots. *Physica A* **216,** 148–150 (1995).
14. Guerin-Pace, F. Rank-size distribution and the process of urban growth. *Urban Stud.* **32,** 551–562 (1995).
15. Robson, B. T. *Urban Growth: An Approach* (Methuen, London, 1972).
16. Theil, H. *Statistical Decomposition Analysis* (North-Holland, Amsterdam, 1972).
17. Batty, M. Entropy in spatial aggregation. *Geogr. Anal.* **8,** 1–21 (1976).
18. Gell-Mann, M. & Tsallis, C. (eds) *Nonextensive Entropy-Interdisciplinary Applications* (Oxford Univ. Press, New York, 2004).
19. Turchin, P. *Historical Dynamics: Why States Rise and Fall* (Princeton Univ. Press, Princeton, New Jersey, 2003).
20. Gabaix, X. Zipf's law for cities: An explanation. *Q. J. Econ.* **114,** 739–767 (1999).
21. Sornette, D. & Cont, R. Convergent multiplicative processes repelled from zero: Power laws and truncated power laws. *J. Phys. I (Paris)* **7,** 431–444 (1997).
22. Pumain, D. in *Hierarchy in Natural and Social Sciences* (ed. Pumain, D.) 169–222 (Springer, Dordrecht, 2006).
23. Gibrat, R. *Les Inégalités Économiques* (Librarie du Recueil, Sirey, Paris, 1931).
24. Malcai, O., Biham, O. & Solomon, S. Power-law distributions and Levy-stable intermittent fluctuations in stochastic systems of many autocatalytic elements. *Phys. Rev. E* **60,** 1299–1303 (1999).
25. Krapivsky, P. L. & Redner, S. Statistics of changes in lead node in connectivity-driven networks. *Phys. Rev. Lett.* **89,** 258703 (2002).

**Supplementary Information** is linked to the online version of the paper at www.nature.com/nature.

**Acknowledgements** This work was partially supported by the EPSRC Spatially Embedded Complex Systems Engineering Consortium. I thank R. Carvalho for useful discussions, and D. Dorling for providing the UK data set.

**Author Information** Reprints and permissions information is available at www.nature.com/reprints. The author declares no competing financial interests. Correspondence and requests for materials should be addressed to the author (m.batty@ucl.ac.uk).